

Local positional and spin symmetry breaking in EuTiO_3 that represent configurations created by two

We consider theoretically the paramagnetic phases of EuTiO_3

sets of microscopic degrees of freedom (mDOFs) positional symmetry breaking due to octahedral rotations and magnetic symmetry breaking due to spin disorder. The effect of these sets of mDOFs on the electronic structure and properties of the para phases is assessed by considering sufficiently large (super)cells with the required nominal global average symmetry, allowing, however, the positional and magnetic symmetries to be lowered. We find that tendencies for local symmetry breaking can be monitored by following total energy lowering in mean-fieldlike density-functional theory, without recourse for strong correlation effects. While most nominally cubic ABO_3 perovskites are known for their symmetry breaking due to the B-atom sublattice, the case of f -electron magnetism in EuTiO_3 is associated with f -sublattice symmetry breaking and its coupling to structural distortions. We find that (i) paramagnetic EuTiO_3 has an intrinsic tendency for both magnetic and positional symmetry breaking, while paramagnetic LaTiO_3 has only magnetic symmetry lowering and no noticeable positional symmetry lowering with respect to low-temperature antiferromagnetic tetragonal phase. (ii) Properly modeled paramagnetic tetragonal and cubic EuTiO_3 have a nonzero local magnetic moment on each Eu ion, consistent with the experimental observations of local magnetism in the para phases of EuTiO_3 significantly above the Néel temperature. Interestingly, (iii) the local positional distortion modes in the short-range ordered para phases are inherited from the long-range ordered low-temperature antiferromagnetic ground-state phase.

DOI: [10.1103/PhysRevMaterials.6.034604](https://doi.org/10.1103/PhysRevMaterials.6.034604)

I. INTRODUCTION

ABO_3 oxide perovskites have attracted significant research

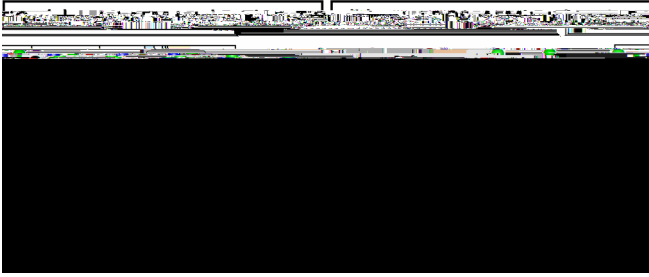


FIG. 1. The α phase of EuTiO_3 : antiferromagnetic tetragonal insulator. (a) Crystal structure of tetragonal EuTiO_3 . (b) The orbital and atom projected density of states (DOS) for AFM-G type tetragonal EuTiO_3

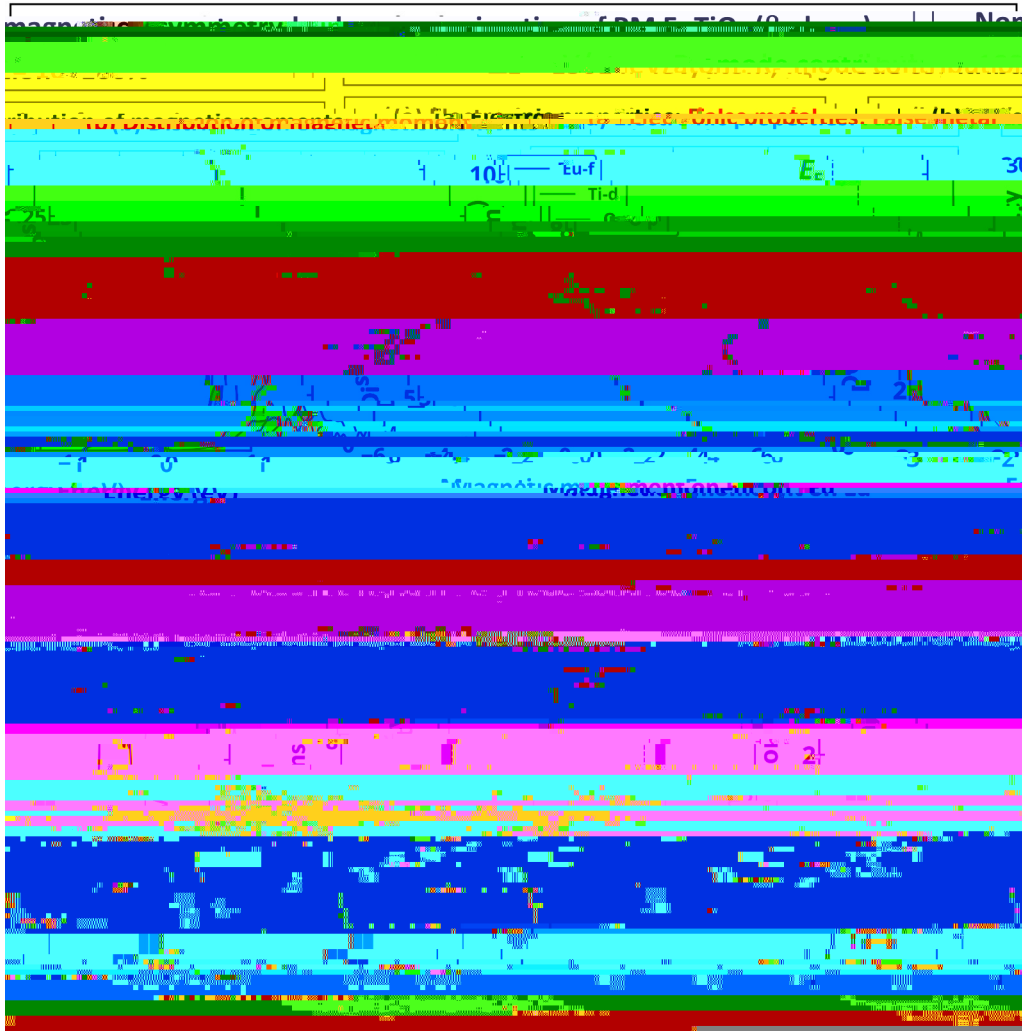


FIG. 2. The β phase of EuTiO_3 : paramagnetic tetragonal insulator. (a), (c) Electronic and (b), (d) magnetic properties of the paramagnetic β phase of EuTiO_3 computed for (a), (b) nonmagnetic symmetry unbroken model and (c), (d) spin polymorphous symmetry broken model. Spin polymorphous symmetry broken model is reproduced by the nudging of 160-atom SQS supercell of tetragonal EuTiO_3 allowing internal

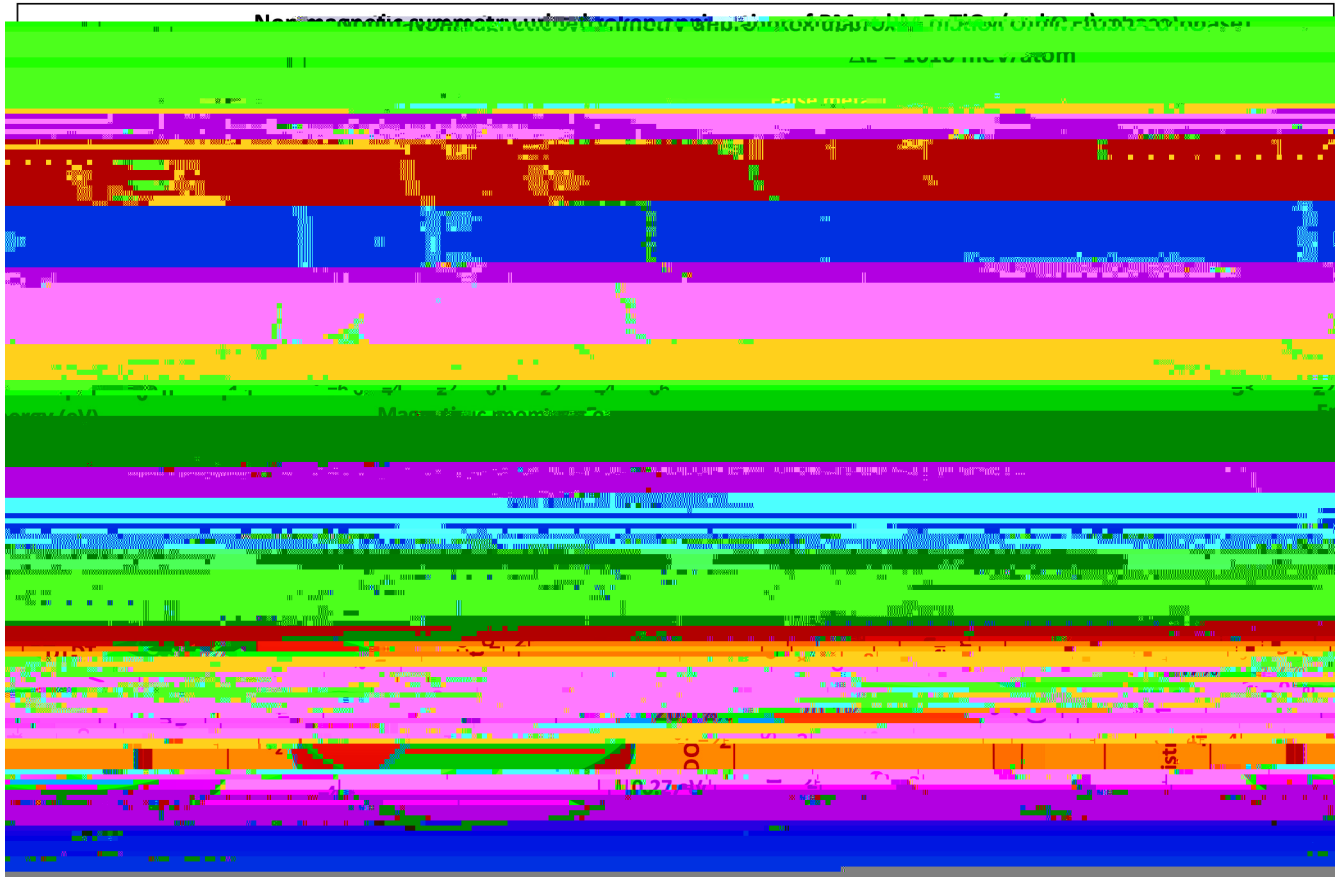


FIG. 3. The γ phase of EuTiO_3 : paramagnetic cubic insulator. (a), (d) Electronic, (b), (e) magnetic, and (c), (f) structural properties of paramagnetic γ phase of EuTiO_3 computed for (a)–(c) nonmagnetic symmetry unbroken model and (d)–(f) spin polymorphous symmetry broken model. The spin polymorphous symmetry broken structure is obtained by the nudging of 160-atom SQS supercell of cubic EuTiO_3 allowing internal relaxation and volume optimization but keeping cubic lattice vectors. The band-gap region in (d) is shown in yellow. The dashed black line in (e) shows the magnetic moments in the α phase. Contribution of different modes to symmetry breaking in paramagnetic γ phase is computed as

